International Journal of Applied Earth Observation and Geoinformation 13 (2011) 165–177

Contents lists available at ScienceDirect

International Journal of Applied Earth Observation and Geoinformation

journal homepage: www.elsevier.com/locate/jag

Validation of a TRMM-based global Flood Detection System in Bangladesh

Caitlin Balthrop Moffitt[a], Faisal Hossain[a,*], Robert F. Adler[b], Koray K. Yilmaz[b], Harold F. Pierce[c]

[a] Department of Civil and Environmental Engineering, Tennessee Technological University, United States
[b] University of Maryland, United States
[c] Laboratory for Atmospheres, NASA Goddard Space Flight Center, Greenbelt, Maryland and Science Systems and Applications, Inc., Lanham, MD, United States

ARTICLE INFO

Article history:
Received 3 March 2010
Accepted 7 November 2010

Keywords:
Satellites
Transboundary flooding
Ungauged basins
Tropical Rainfall Measuring Mission
Rainfall
Ground validation

ABSTRACT

Although the TRMM-based Flood Detection System (FDS) has been in operation in near real-time since 2006, the flood 'detection' capability has been validated mostly against qualitative reports in news papers and other types of media. In this study, a more quantitative validation of the FDS over Bangladesh against in situ measurements is presented. Using measured stream flow and rainfall data, the study analyzed the flood detection capability from space for three very distinct river systems in Bangladesh: (1) Ganges–a snowmelt-fed river regulated by upstream India, (2) Brahmaputra – a snow-fed river that is braided, and (3) Meghna – a rain-fed and relatively flashier river. The quantitative assessment showed that the effectiveness of the TRMM-based FDS can vary as a function of season and drainage basin characteristics. Overall, the study showed that the TRMM-based FDS has great potential for flood prone countries like Bangladesh that are faced with tremendous hurdles in transboundary flood management. The system had a high probability of detection overall, but produced increased false alarms during the monsoon period and in regulated basins (Ganges), undermining the credibility of the FDS flood warnings for these situations. For this reason, FDS users are cautioned to verify FDS estimates during the monsoon period and for regulated rivers before implementing flood management practices. Planned improvements by FDS developers involving physically-based hydrologic modeling should transform the system into a more accurate tool for near real-time decision making on flood management for ungauged river basins of the world.

1. Introduction

Although water is essential to life, its excess (i.e., flooding) can cause major damage and loss of life. Since 1970, more than 7000 major flooding and drought events have caused approximately $2 trillion in damages and 2.5 million in casualties (World Water Assessment Programme, 2009). Among the many types of flooding, transboundary flooding occurs when floodwaters move along an international river from an upstream nation to a nation downstream. When high rainfall accumulation occurs in upstream nations and is not communicated to downstream nations in near real-time, it becomes challenging for downstream nations to manage the flooding. While transboundary river floods only represent 9.9% of all flooding events, they account for 32% of all casualties, almost 60% of affected individuals, and 14% of financial damage (Bakker, 2006). The disproportionate relationship between occurrence and impact with transboundary floods is primarily due to the lack of communication between countries regarding rainfall and the ensuing stream flow data for flood monitoring purposes (Balthrop and Hossain, 2010).

The challenges with near real-time data communication are often attributed to a lack of ground infrastructure and data sharing treaties between nations along the same river reach. Many nations have a declining a ground network or lack the infrastructure necessary to gauge their rivers and monitor rainfall (Stokstad, 1999). In the United States, ground gauging is also declining due to a lack of resources and maintenance (Wahl et al., 1995). For countries with some ground-measured data, there is often a lack of communication among riparian nations due to absence of a cooperative mechanism (Bakker, 2006). A comprehensive review of freshwater treaties on flooding has shown that there currently exists no treaty that addressed the sharing of measured stream flow or rainfall data in near real-time among riparian nations of an international river basin (Balthrop and Hossain, 2010).

A solution to the challenges of near real-time hydrologic data communication is to leverage a space-borne platform for data collection. The vantage of space overcomes any political hurdles on the ground by providing estimates that are freely accessible on both sides of the border. The space vantage also offers an opportunity for more frequent and denser sampling because the data no longer has to rely on sparsely deployed or declining ground infrastructure, but rather on the spatial and temporal resolution of the satellite orbits.

* Corresponding author at: Department of Civil and Environmental Engineering, Tennessee Technological University, 1020 Stadium Drive, Box 5015, Cookeville, TN 38505-0001, United States. Tel.: +1 931 372 3257; fax: +1 931 372 6239.
E-mail address: fhossain@tntech.edu (F. Hossain).

0303-2434/$ – see front matter © 2010 Elsevier B.V. All rights reserved.
doi:10.1016/j.jag.2010.11.003

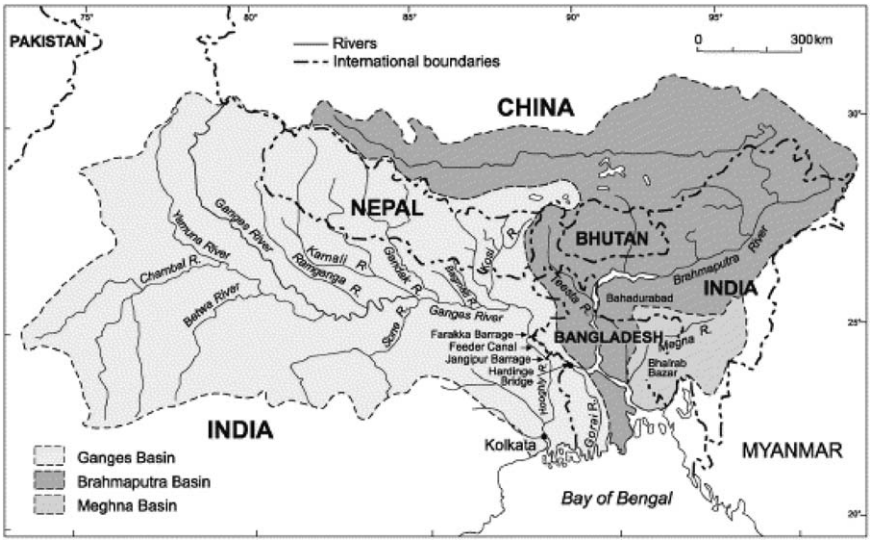

Fig. 1. Ganges–Meghna–Brahmaputra river basin.

Currently, NASA has in operation the Tropical Rainfall Measurement Mission (TRMM), a satellite mission that utilizes a microwave imager and the first space-borne precipitation radar to estimate rainfall (Simpson et al., 1988; Kummerow et al., 2000). Although this satellite is limited to an orbit in the tropics (35°N–35°S), it is the calibration focal point for a constellation of satellites used to derive satellite rainfall products known as the TRMM Multi-satellite Precipitation Analysis (TMPA). TMPA provides rainfall products in 3 h increments for $0.25^\circ \times 0.25^\circ$ grids across most of the globe (Huffman et al., 2007) and is a pathfinder to optimal products for the Global Precipitation Measurement (GPM) Mission. The GPM is scheduled to replace TRMM in 2013 and will utilize instrumentation similar to that onboard TRMM but provide rainfall estimates for the entire globe (Hou et al., 2008).

There can many different ways to monitor flood and perform flood risk assessment on a global scale. For example, flood monitoring can be achieved through rain-based systems, where the rain being monitored by space borne sensors are fed into a global hydrologic model for deriving the flood potential (Hong et al., 2007). Another way of flood monitoring can be based on the direct detection surface water inundation from remote sensing platforms, such as the Dartmouth Flood Observatory (Brackenridge et al., 2005) and the JRC Global Flood Detection System. Some examples of rain-based systems include the Global Flood Alert System (GFAS; Kera and Nagai, 2006) and the Ithaca Early Warning System. [Here ITHACA is the acronym for **I**nformation **T**echnology for **H**umanitarian **A**ssistance, **C**ooperation and **A**ction (see http://ithaca.polito.it)]. There is another class of system that use rainfall forecast to produce flood forecasts with a few days of lead time (such as the European Flood Alert System that uses the forecast rainfall produced by the European Center for Medium Range Weather Forecasting – ECMWF).

This study focuses on flood monitoring based on satellite rainfall estimation and its hydrologic modeling to compute the surface runoff. From the simplest hydrologic model to the most complex, rainfall is the key input that drives the accuracy of the runoff output necessary for flood forecasting. Recently, the TMPA-based rainfall has been incorporated into a near real-time hydrologic model that determines the runoff depth generated along a calculated flow path with a metric value for flood potential. This system is known as the TRMM-based Flood Detection System (FDS) (Hong et al., 2007).

The TRMM-based FDS utilizes dynamic satellite-based rainfall along with topography, land cover, and soil property data in a hydrologic model to determine areas of flood risk for 50°N–50°S (Hong et al., 2007). The FDS system implements the Natural Resources Conservation Service (NRCS)-Curve Number (CN) model to generate runoff depth, and from that data areas of flood risk (Hong and Adler, 2008). For this model, it is important to have a constant streaming of the rainfall information to capture the dynamics of flooding. Properties like topography, land cover, and soil properties are generally unchanged at daily timescales or vary seasonally, and hence, do not require a continuous update. For this reason, the TRMM-based FDS can only be as accurate as its dynamic input, which is why validation of this input along with its output (i.e., prediction) is necessary.

Because the FDS has only been in operation since 2006, there is not much work in literature that demonstrates the performance of the system against in situ measurements. Yet, the continuous watch on floods around the globe by the FDS has tremendous potential for benefitting society where such information is sparse. In the most recent flood damage by Cyclone Nargis over Myanmar in 2008, it was reported that the Red Cross used FDS output to help identify flooded areas and plan mitigation actions. Hence, validation of the FDS is important because understanding the effectiveness of the system is essential to optimizing its performance and to making future model improvements. Qualitative validation is often performed for extreme events on the TRMM website (NASA, http://trmm.gsfc.nasa.gov/publications_dir/extreme_events.html), but quantitative validation is necessary to understand the magnitude of uncertainty associated with FDS output flood data. It is this uncertainty that ultimately affects the decision-making process.

There have been efforts to validate the TMPA-based rainfall input for the FDS and implement it into different hydrologic models, such as the Xinanjiang Model (Li et al., 2008) and the Variable Infiltration Capacity (VIC) model (Su et al., 2008). However, to the best of our knowledge, no quantitative validation has been done for the FDS to determine the effectiveness of the NRCS-CN-based flood potential output.

In this study we have selected Bangladesh as the study region for validation because of the widespread transboundary flooding it experiences. The objectives of this study are: (1) to determine how effectively a TMPA-based rainfall product senses rainfall events and

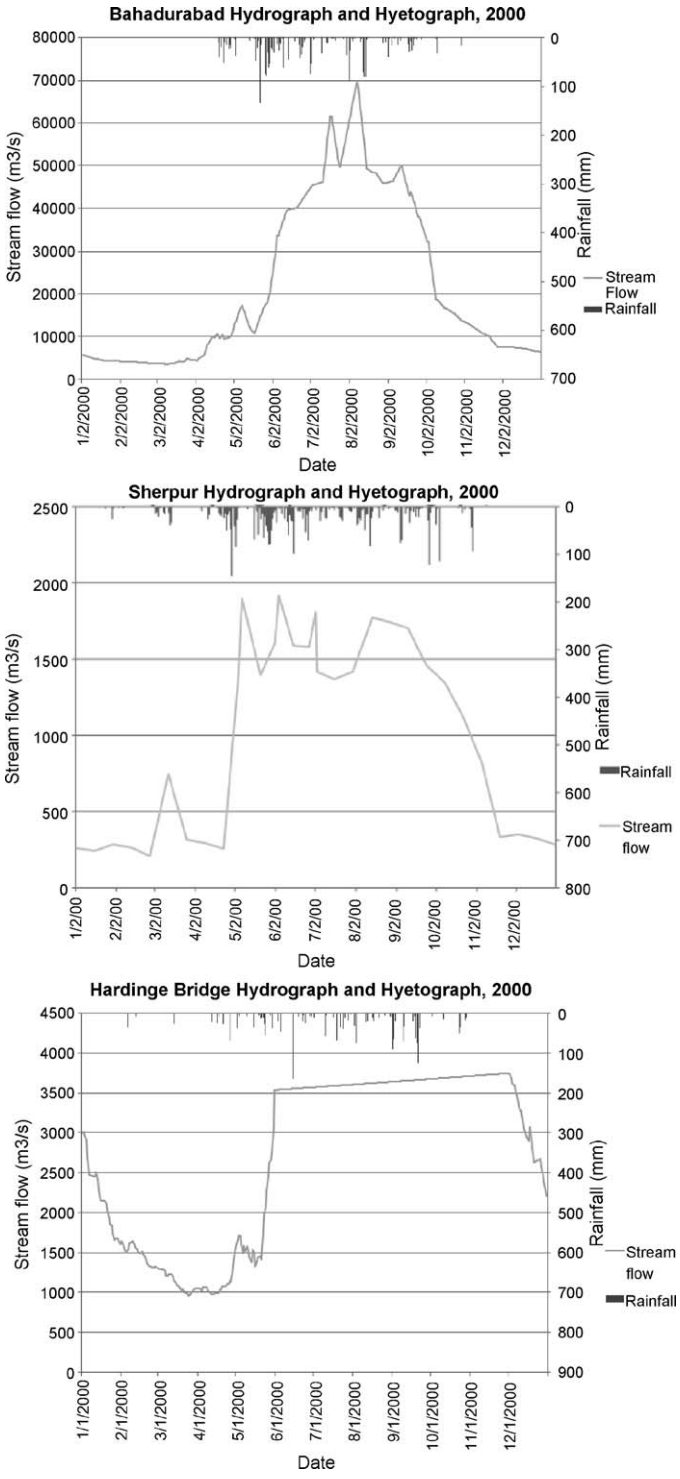

Fig. 2. (a) Bahadurabad hydrograph and hyetograph for 2000 (Brahmaputra River), (b) Sherpur hydrograph and hyetograph for 2000 (Meghna River), (c) Hardinge bridge hydrograph and hyetograph for 2000 (Ganges River).

estimates their magnitude, and (2) to determine how effectively the TRMM-based FDS detects flood events and their magnitude.

This paper is organized as follows. In Section 2, the study region and data used in this analysis are discussed. Section 3 outlines the methodology for the rainfall and flood potential validations; followed by Section 4, which is a discussion of the results. Conclusions are presented in Section 5, which also discusses limitations of the study and presents suggestions for future work.

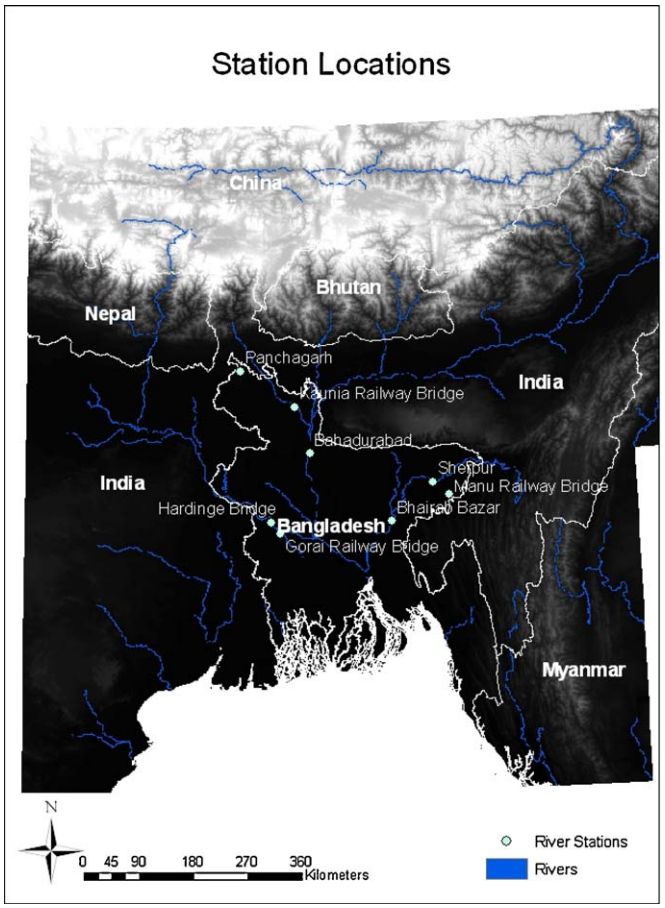

Fig. 3. Ground validation station location map (for stream gauging).

2. Study region and data

2.1. Study region: Bangladesh

Bangladesh is home to the largest river delta in the world, the confluence of the Ganges, Meghna, and Brahmaputra rivers (Fig. 1). This area experiences annual flooding during the monsoon season lasting from June through October, generating 85% of the country's total annual runoff. The combined annual runoff of these three rivers is 1230 billion cubic meters (Ahmad et al., 2001), a flow which is only exceeded by the annual discharge of the Amazon and Congo Rivers (Hopson and Webster, 2009).

Bangladesh has three major and distinct river systems within its borders (Fig. 2). The Ganges River originates at the Gangotri glaciers in the Himalayas and along its 2500 km reach passes through Nepal, China, and India and empties into the Bay of Bengal at Bangladesh. Of the 980,000 km^2 drainage basin, only 34,188 km^2 (3.6%) lies within Bangladesh (Islam et al., 1999). The Ganges River is regulated as it passes through India, with a large diversion structure, the Farakka Barrage, just 17 km upstream from the Bangladesh border (Rahaman, 2005). The Brahmaputra River also begins in the glaciers of the Himalayas and travels 2896 km through China, Bhutan, and India before emptying into the Bay of Bengal in Bangladesh. Of the 640,000 km^2 drainage area, only 50,505 km^2 (8.7%) lies within Bangladesh (Islam et al., 1999). For a river of its size, it is impressive that it remains a natural stream with no major hydraulic structures built along its reach (Rahaman, 2005). The Meghna River is a comparatively smaller, rain-fed, and relatively flashier river that runs through a mountainous region in India before enter-

Table 1
Tabular summary of datasets.

Measure	Type	Units	Frequency	Resolution
TRMM (satellite)	Rainfall	mm	3 h	0.25 × 0.25°
TRMM (satellite)	Flood potential	mm	3 h	0.25 × 0.25°
Gauge (ground)	Rainfall	mm	Daily	Point
Gauge (ground)	Streamflow	m^3/s	Daily	Point

Table 2
River stations sorted by upstream drainage area.

Station	Upstream drainage area (km^2)
Hardinge Bridge	875,613.92
Bahadurabad	405,107.96
Bhairab Bazar	64,848.01
Sherpur	35,892.14
Kaunia Railway Bridge	10,649.49
Gorai Railway Bridge	8804.59
Manu Railway Bridge	2314.87
Panchagarh	487.20

Table 3
The 2 × 2 contingency table.

		Satellite	
		Detected	Not detected
Ground	Observed	Hit	Miss
	Not observed	False alarm	Null

ing Bangladesh. Of the 85,000 km^2 drainage area, only 36,000 km^2 (42.4%) lies within Bangladesh.

Because the majority of the Ganges, Brahmaputra, and Meghna river basin drainage areas are comprised of the nations surrounding Bangladesh, approximately 90% of the flow is transboundary (Rahaman, 2005). Bangladesh lacks and adequate water treaty with upstream nations (Hossain and Katiyar, 2006) and the current lead time for flood forecasting within the country's borders is 2–3 days using traditional ground-based measurements (Paudyal, 2002). Hossain and Katiyar (2006) argue that the lead time could be improved because the Ganges, Meghna, and Brahmaputra river basins have a mean basin rainfall response time of 7–14 days. Satellite rainfall and flood data, like that available through TRMM and the FDS, could help to increase the flood forecasting lead time by detecting areas at risk for flooding. For this reason, Bangladesh is an ideal location for validation of the TRMM-based FDS.

2.2. TRMM-based Flood Detection System

The TRMM-based FDS utilizes a near real-time TMPA-based rainfall product and incorporates it into a hydrologic model to determine areas of flood risk for regions bounded by 50°N and 50°S (Hong et al., 2007). The simple hydrologic model used for the system is the Natural Resources Conservation Service (NRCS)-Curve Number (CN). This model utilizes the dynamic rainfall input along with topography, land use, and hydrologic condition data to determine a time-varying CN for a given grid box. Precipitation record of preceding days is used as a proxy for soil wetness for the day to day determination of the CN for each grid box. This CN then dictates how much of the rainfall is partitioned as direct runoff. This model is used to generate direct runoff because it can produce results in near real-time with little computation (Hong and Adler, 2008).

3. Datasets

3.1. TMPA version 6 (V6) rainfall data

The TMPA V6 rainfall data are the post-near real-time research quality rainfall data derived from TRMM. They are produced as the depth of rainfall for a 0.25° × 0.25° grid box (Huffman et al., 2007). Also known as 3B42V6 (hereafter), this rainfall data incorporate ground-based monthly gauge data to minimize the bias of precipitation (Huffman et al., 2007). The data used in this study were available in 3 h increments for the study period of January 1, 2000–December 31, 2005. To account for the fact that the satellite

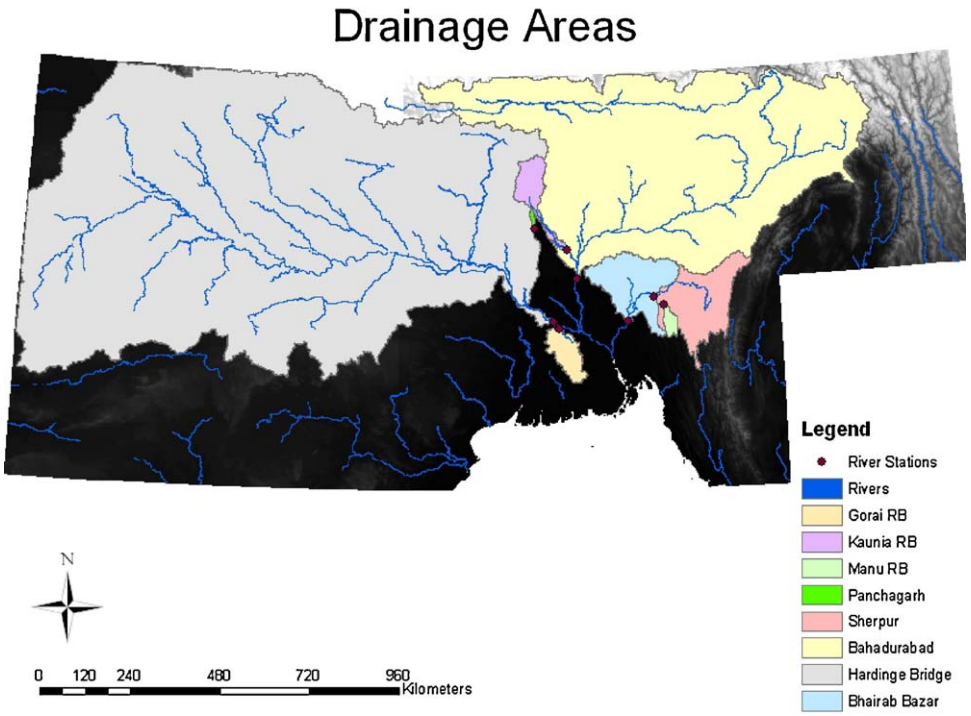

Fig. 4. Drainage area maps for each stream gauging station. Drainage areas were determined using topography data from the SRTM website at a 90 m resolution.

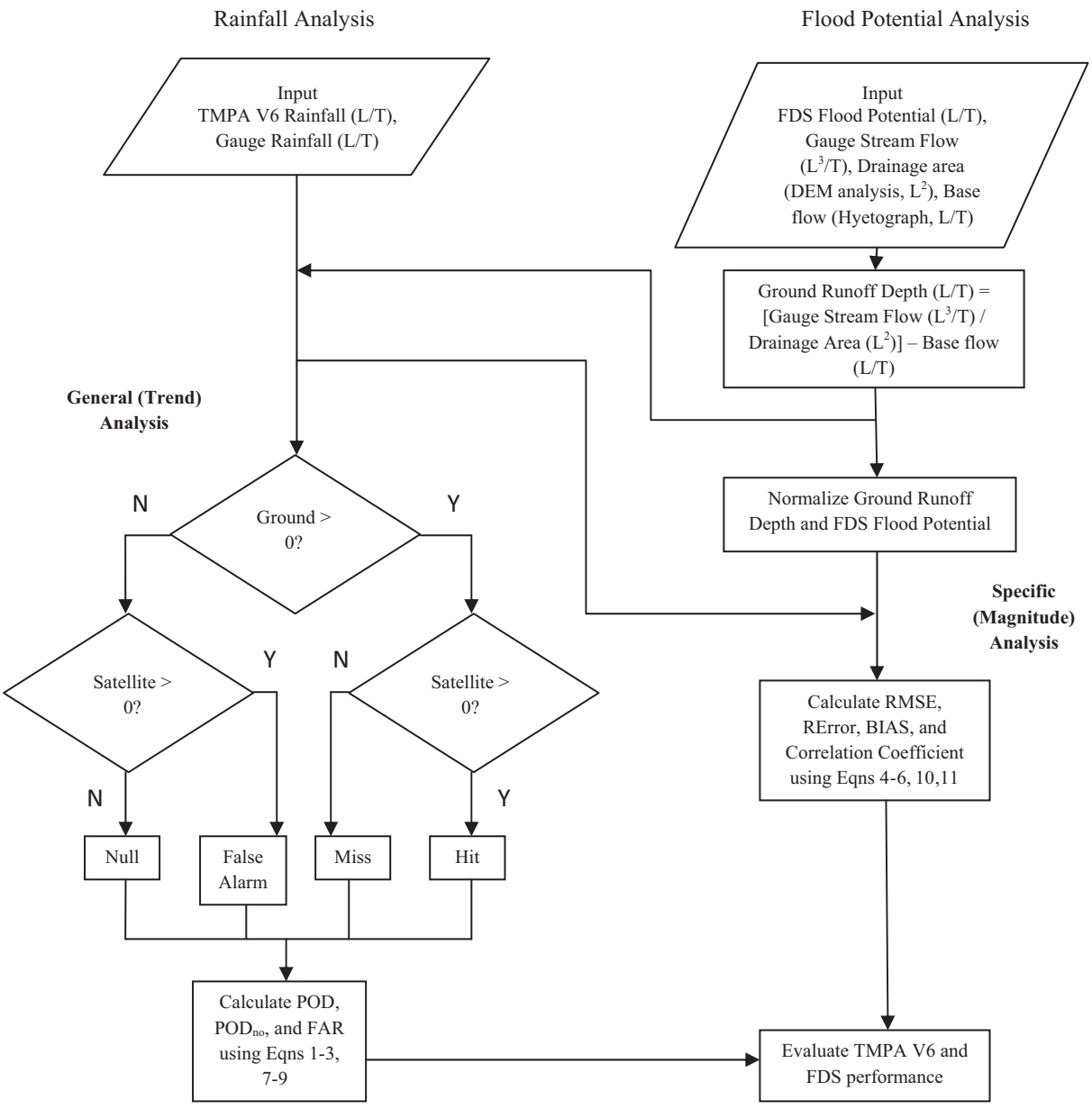

Fig. 5. Methodology flowchart.

rainfall data are gridded and not point locations like ground measurements, the grid boxes surrounding the stations (Fig. 3) were used for the validation study (Table 1).

3.2. TRMM-based FDS flood potential data

The TRMM-based FDS flood potential data are estimates of the average runoff depth for a $0.25^\circ \times 0.25^\circ$ grid. For the region of Bangladesh, this translates into an approximately 25 km × 25 km grid box, varying slightly at different latitudes within the country. The data were available in 3 h increments in the tropics from January 1, 2000 to December 31, 2005. Just like rainfall, only the grid boxes surrounding the stream flow gauging stations (Fig. 3) were used in this study.

3.3. Ground rainfall data

Because rainfall data were not available at the exact location of each stream gauging stations (Fig. 3), data from the nearest (to stream gauge) were used within the corresponding TMPAV6 rainfall grid box. Rainfall data were available at the daily timescale from 2000 to 2005. It should be kept in mind that the rain gauge data are for the lower part of the basins, which are in Bangladesh, and do not represent the upstream part of the basins.

3.4. Ground stream gauge data

The ground stream flow data were available at each of the stations along major rivers within Bangladesh (Fig. 3). The data were available at daily timescales from 2000 to 2005. Where there were occasional small gaps in data, values were interpolated.

4. Methodology

For this study, eight river stations were selected in Bangladesh within the drainage areas of each river basin (Fig. 3). For the Ganges basin, sites included the Hardinge Bridge and the Gorai Railway Bridge. For the Brahmaputra basin, sites at Bahadurabad, Kaunia

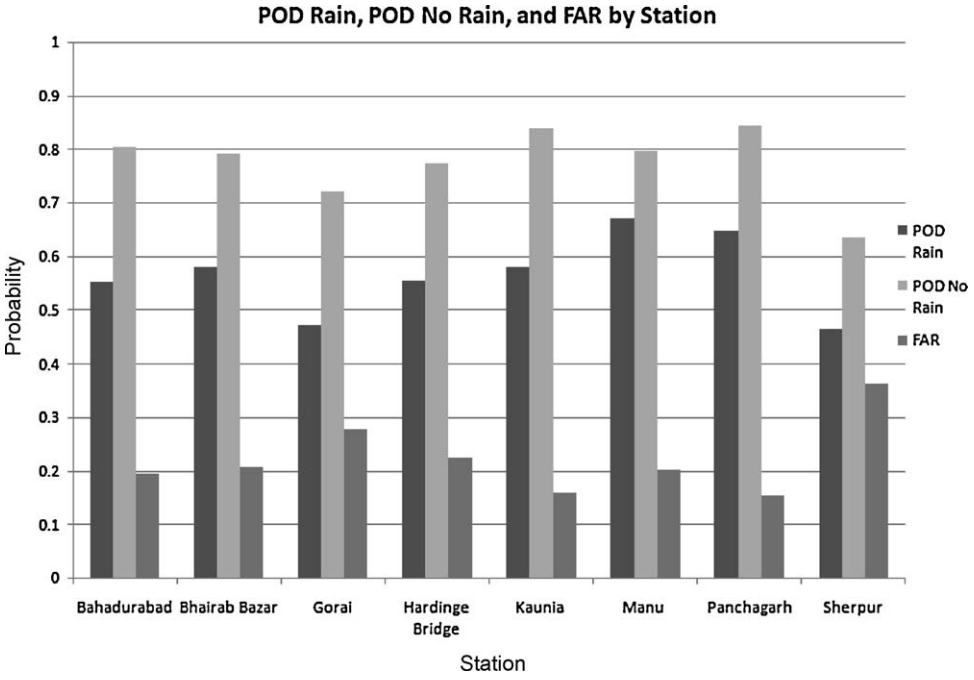

Fig. 6. POD_{rain}, $POD_{no\ rain}$, and FAR_{rain} by station.

Railway Bridge and Panchagarh were analyzed. The Meghna basin was analyzed at the Bhairab Bazar, Sherpur, and Manu Railway Bridge sites.

The four datasets outlined in the previous section were used for validation. Because the output of the FDS (runoff depth) was in units of depth per unit time (mm/3 h) and the corresponding ground stream flow data were in units of volume per unit time (m^3/s), direct validation by comparison presented a challenge. In order to directly compare the ground datasets at each station for analysis with the FDS output, the units were converted for compatibility. This was done by dividing the ground stream flow data by the upstream drainage area and removing 'base flow' component to determine the depth of direct runoff on the ground. Base flow was separated by identifying an average dry season flow for a non-rainy period of one month and then subtracting that from the stream flow hydrograph. The drainage area was obtained using digital elevation model (DEM) files from the NASA Shuttle Radar Topography Mission (SRTM) website (CGIAR Consortium for Spatial Information, http://srtm. csi.cgiar.org/). These DEMs were then analyzed to determine the routing characteristics

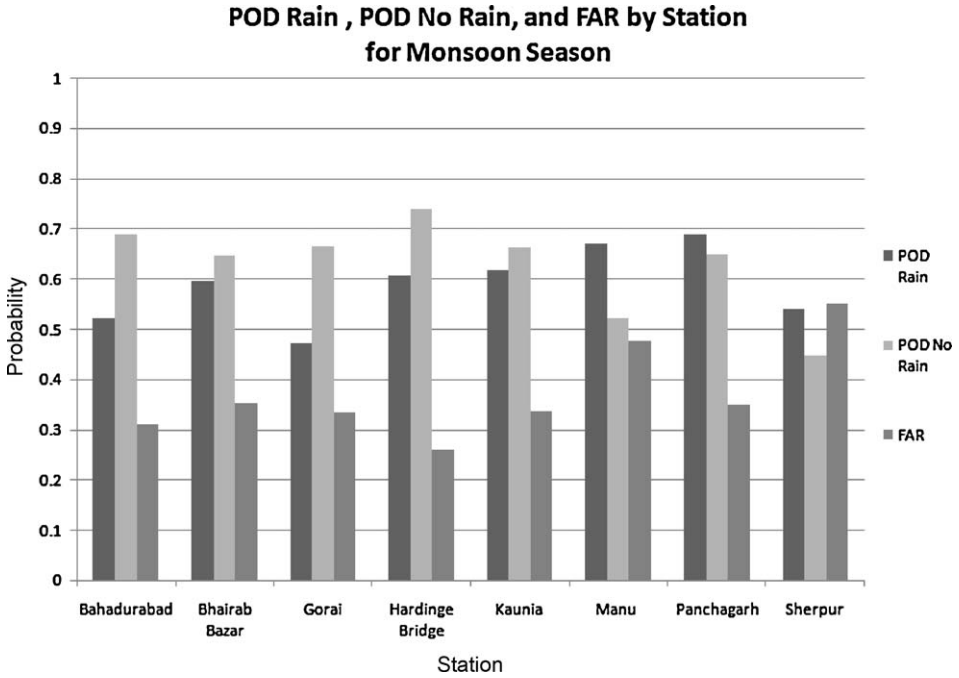

Fig. 7. POD_{rain}, $POD_{no\ rain}$, and FAR_{rain} by station for Monsoon season.

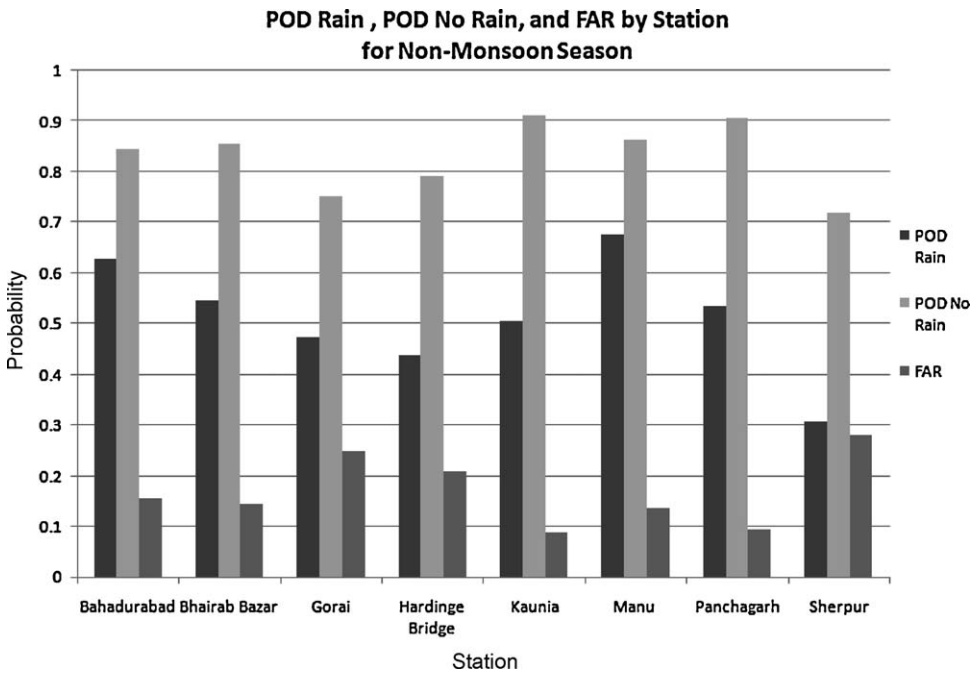

Fig. 8. POD_{rain}, $POD_{no\ rain}$, and FAR_{rain} by station for Non-Monsoon season.

for each drainage basin, including the drainage area (see Fig. 4 and Table 2).

Fig. 5 summarizes the overall methodology approach in the form a flowchart. The analysis was divided into two components, a rainfall analysis and a flood potential analysis. Both analyses followed a similar strategy in which a general "trend" evaluation was performed to determine how well the satellite system detected patterns in gauge data. The analysis then became more specific, and presented how well the satellite system estimated the scalar magnitude of events. All comparisons of rainfall and runoff data were done at the daily timescale.

4.1. Rainfall analysis

The first part of the rainfall analysis determined how effectively the TMPA-based rainfall product detected patterns in ground rainfall data. This was evaluated using a 2×2 contingency table in which the cells represent a hit, miss, false alarm, or null event (Table 3). From the contingency table analysis, the following metrics were calculated for rainfall: Probability of Detecting Rainfall (POD_{rain}; Eq. (1), Probability of Detecting No Rainfall ($POD_{no\ rain}$; Eq. (2), and False Alarm Ratio of Rainfall (FAR_{rain}; Eq. (3). Other rainfall validation studies may define FAR differently (Ebert et al.,

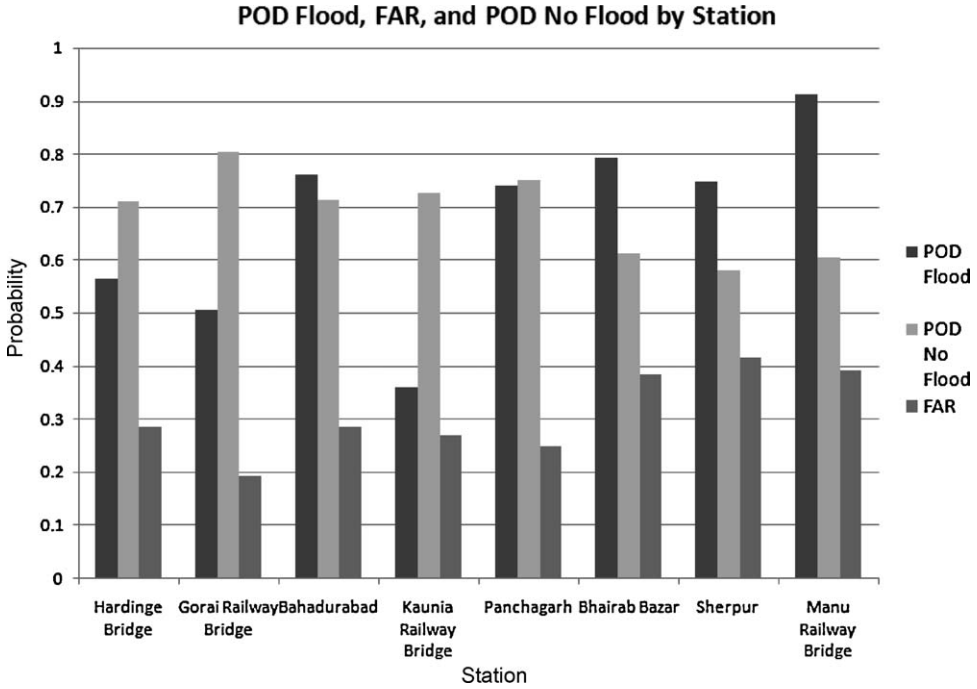

Fig. 9. POD_{flood}, $POD_{no\ flood}$, and FAR_{flood} by station.

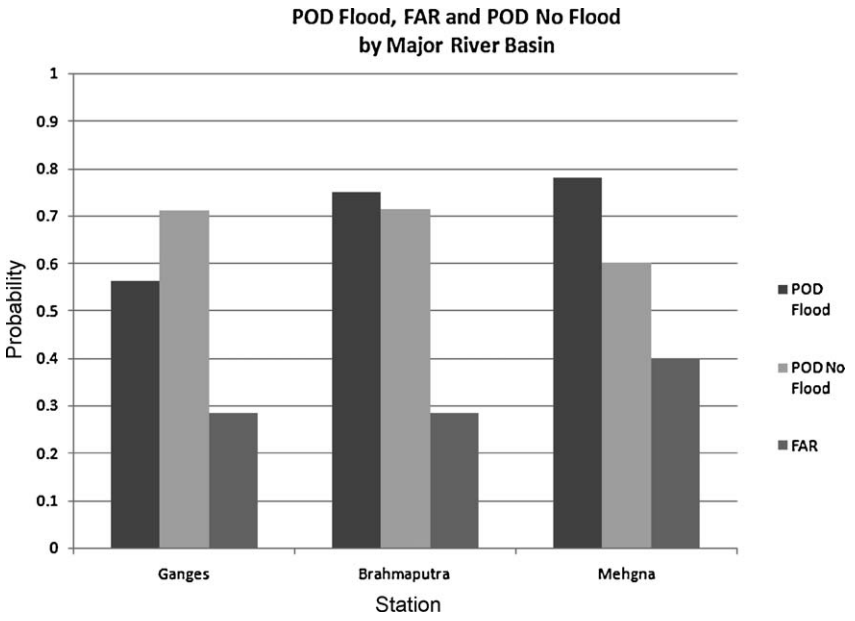

Fig. 10. POD_{flood}, $POD_{no\ flood}$, and FAR_{flood} by river basin.

2007; Su et al., 2008), so it is important to note the difference in this study.

$$POD_{no\,rain} = \frac{Hits_{rain}}{Hits_{rain} + Misses_{rain}} \quad (1)$$

$$POD_{no\,rain} = \frac{Nulls_{rain}}{Nulls_{rain} + False\ alarms_{rain}} \quad (2)$$

$$FAR_{no\,rain} = \frac{False\ alarms_{rain}}{Nulls_{rain} + False\ alarms_{rain}} \quad (3)$$

These metrics were computed for each station for the entire data period (2000–2005) and then separately for the monsoon (flooding season) and non-monsoon (dry season) seasons to determine how well the system performed during periods of contrasting rainfall patterns. The analysis as a function of seasons is expected to help FDS decision-makers and model developers understand the reliability of flood risk maps generated by the TRMM-based system during periods of widespread rainfall and during periods of infrequent rainfall.

The purpose of the second part of the rainfall analysis was to understand how effectively 3B42V6 'sensed' the magnitude of rainfall events. The datasets were compared for the entire time period (unconditional) and then isolated to consider the hits (conditional). Using the converted ground rainfall and the satellite rainfall, rela-

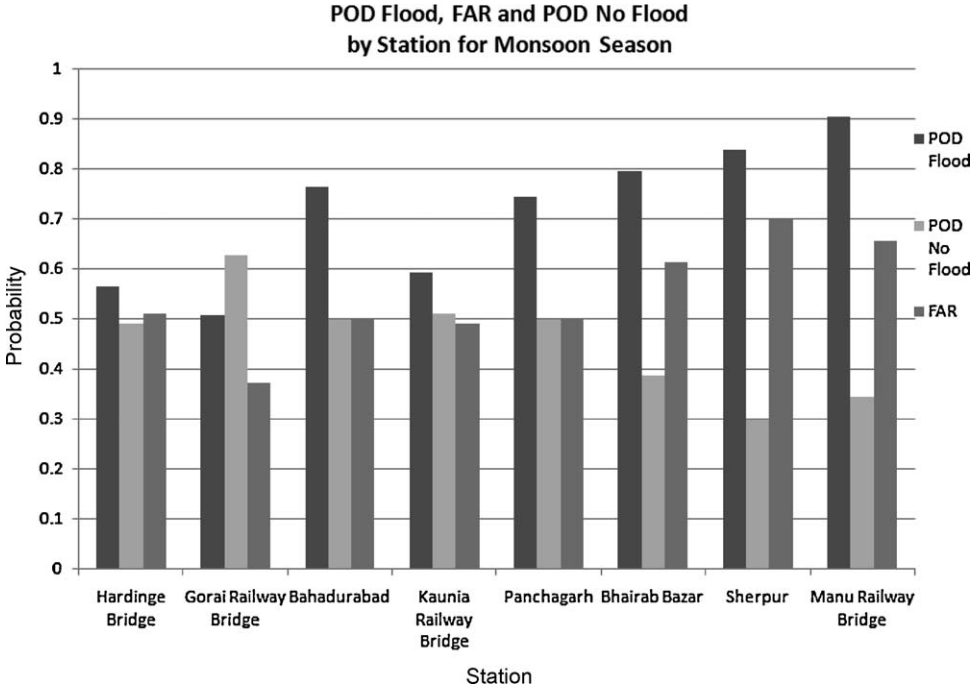

Fig. 11. POD_{flood}, $POD_{no\ flood}$, and FAR_{flood} by station for Monsoon season.

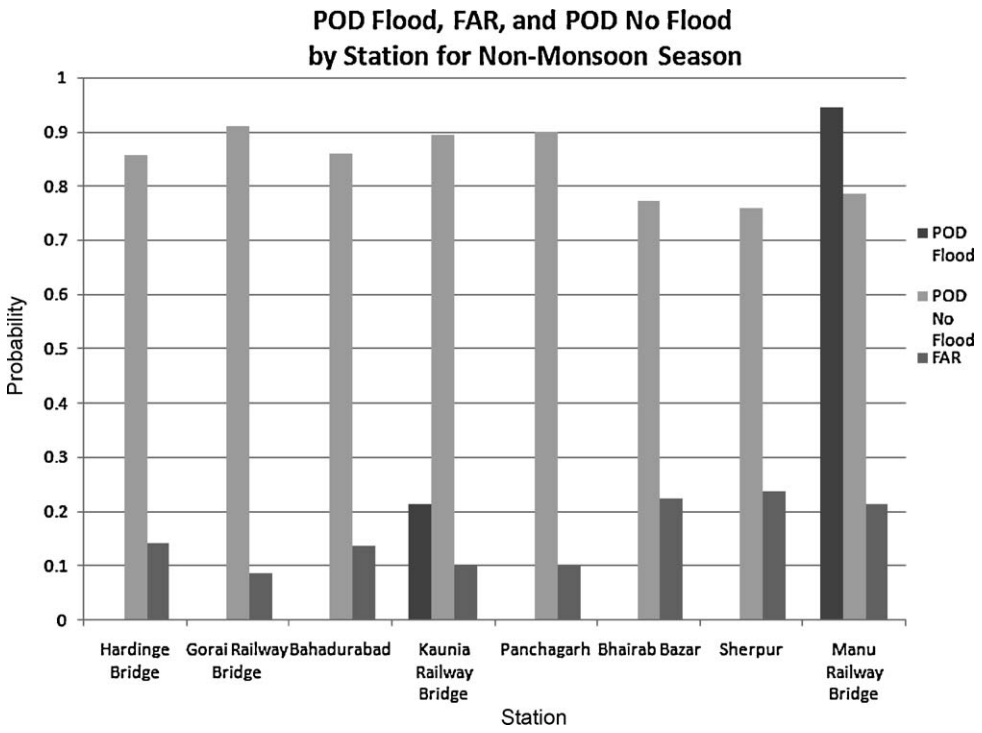

Fig. 12. POD_{flood}, $POD_{no\ flood}$, and FAR_{flood} by station for non-Monsoon season.

tive root mean square error (RRMSE; Eq. (4)), bias (Eq. (5)), and correlation coefficient (r_{sg}; Eq. (6)) were determined at each of the stations.

$$\mathrm{RRMSE_{rain}} = \frac{\sqrt{\sum_{i=1}^{N}(R_g - R_g)^2}}{\sum_{i=1}^{N} R_g/N} \tag{4}$$

where R_s is satellite rainfall depth in mm/d and R_g is ground rainfall depth in mm/d, i is an integer, and N is the total number of data points.

$$\mathrm{Bias_{rain}} \frac{\sum R_s}{\sum R_g} \tag{5}$$

$$r_{sg}(\mathrm{Rainfall}, R) = \frac{\sum_{i=1}^{N}(R_s - \bar{R}_s)(R_g - \bar{R}_g)}{(N_s - 1)\sigma_{RS}\sigma_{Rg}} \tag{6}$$

where $\bar{R}_s$ is the mean of the satellite rainfall depth, $\bar{R}_g$ is the mean of the ground rainfall depth, σ_{Rs} is the standard deviation of the satellite rainfall depth, and σ_{Rg} is the standard deviation of the ground rainfall depth.

4.2. Flood potential analysis

The first part of the flood potential analysis determined how effectively the FDS detected the patterns observed from ground data. Flood events from ground stream flow data were determined as those events above the 98th percentile of all stream flow events for the 2000–2005 time period. These values were determined by plotting flow duration curves, or the magnitude of the flood against the probability that that flood magnitude was met or exceeded. For satellite flood potential and ground stream flow data, when a flood event occurred it was assigned a value of "1." If no flood occurred, then it was assigned a value of "0." The two sets of data were then compared using a 2×2 contingency table in which the cells represent a hit, miss, false alarm, or null event (Table 2). From the contingency table analysis, the following metrics were calculated for flood potential: Probability of Detecting Flooding (POD_{flood}; Eq. (7)), Probability of Detecting No Flooding ($POD_{no\ flood}$; Eq. (8)), and False Alarm Ratio of Flooding (FAR_{flood}; Eq. (9)).

$$\mathrm{POD_{flood}} = \frac{\mathrm{Hits_{flood}}}{\mathrm{Hits_{flood}} + \mathrm{Misses_{flood}}} \tag{7}$$

$$\mathrm{POD_{no\,flood}} = \frac{\mathrm{Nulls_{flood}}}{\mathrm{Nulls_{flood}} + \mathrm{False\ alarms_{flood}}} \tag{8}$$

$$\mathrm{FAR_{flood}} = \frac{\mathrm{False\ alarms_{flood}}}{\mathrm{Nulls_{flood}} + \mathrm{False\ alarms_{flood}}} \tag{9}$$

The data were also separated into monsoon and non-monsoon seasons to determine how the system performed during periods of contrasting stream flow patterns (consistently high flows in the monsoon season and lower flows in the non-monsoon season). These metrics were considered by station, by major river basin and by station during the monsoon and non-monsoon seasons to determine how well the system performed in each scenario.

The FDS drainage areas are based on coarse Hydro1K data (Hong et al., 2007) whereas this analysis used the higher resolution SRTM topography data. To minimize the inconsistencies in resolution of these databases, the ground and satellite runoff depth values were both normalized by subtracting the mean value and dividing by the standard deviation. Scattergrams were then generated to determine how far off from the line of perfect agreement the two sets of data were.

Next, the total dataset (unconditional) was considered as well as the hits (conditional). These were separately analyzed for bias (Eq. (10)), and correlation coefficient (Eq. (11)) to determine how effectively the satellite sensed the magnitude of flood events.

$$\mathrm{Bias_{flood}} = \frac{\Sigma F_s}{\Sigma F_g} \tag{10}$$

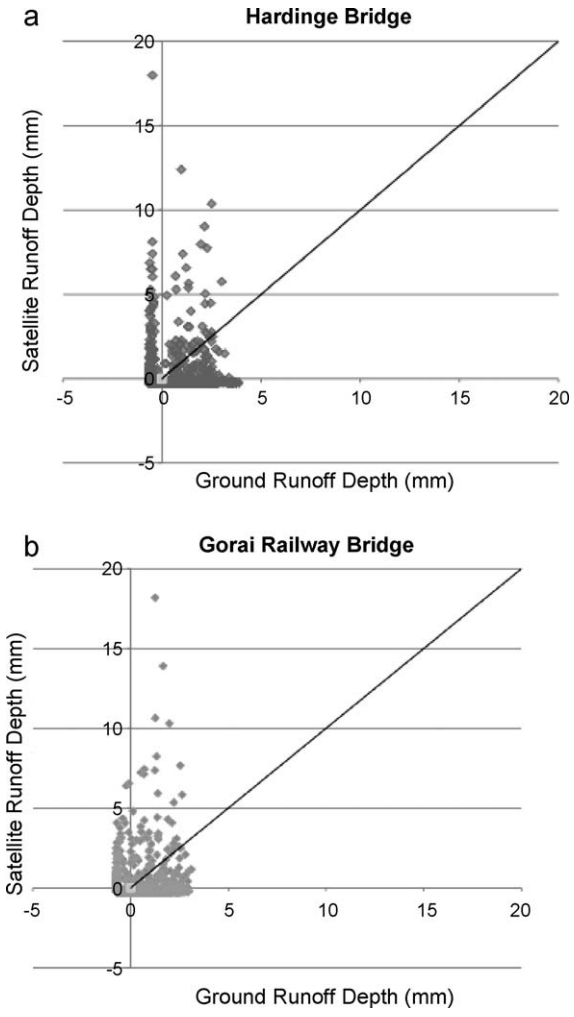

Fig. 13. Scattergrams for the Ganges river basin stations.

where F_s is satellite runoff depth in mm/d and F_g is ground runoff depth in mm/d.

$$r_{sg}(\text{Flood potential},\ F) = \frac{\sum_{i=1}^{N}(F_s - \bar{F}_s)(F_g - \bar{F}_g)}{(N-1)\sigma_{FS}\sigma_{Fg}} \tag{11}$$

where $\bar{F}_s$ is the mean of the satellite runoff depth, $\bar{F}_g$ is the mean of the ground runoff depth, σ_{Fs} is the standard deviation of the satellite runoff depth, and σ_{Fg} is the standard deviation of the ground runoff depth.

5. Results and discussions

When reviewing the results of these analyses, it is important to consider that validation was done for a satellite grid with an approximate area of 625 km^2 using point gauge data as the ground "truth." Also, where ground data were missing, values were interpolated between known values. Therefore, there is a level of uncertainty associated with data that could inflate error estimates. Although we expect this to be minimal, a different set of in situ data with higher resolution (within a TMPA grid box) measurements may possibly yield different results.

5.1. Rainfall analysis

The rainfall analysis sought to determine how well the 3B42V6 estimated trends and the magnitude of rainfall on the ground. Overall, average results (across all stations) showed high POD_{rain} (0.57) and $POD_{no\ rain}$ (0.78) indicating that the TMPA system can be quite effective in estimating rainfall trends in the ground data (Fig. 6). Ebert et al. (2007) have shown similar results in POD_{rain} for Europe (0.56) and for Australia (0.54) using modeled rainfall for validation studies. The FAR_{rain} (0.22) represented an inherent uncertainty with the 3B42V6 rainfall estimates in falsely detecting rainfall when it did not occur on the ground, although this result is probably related partially to the area satellite estimate versus the point gauge estimate of rain.

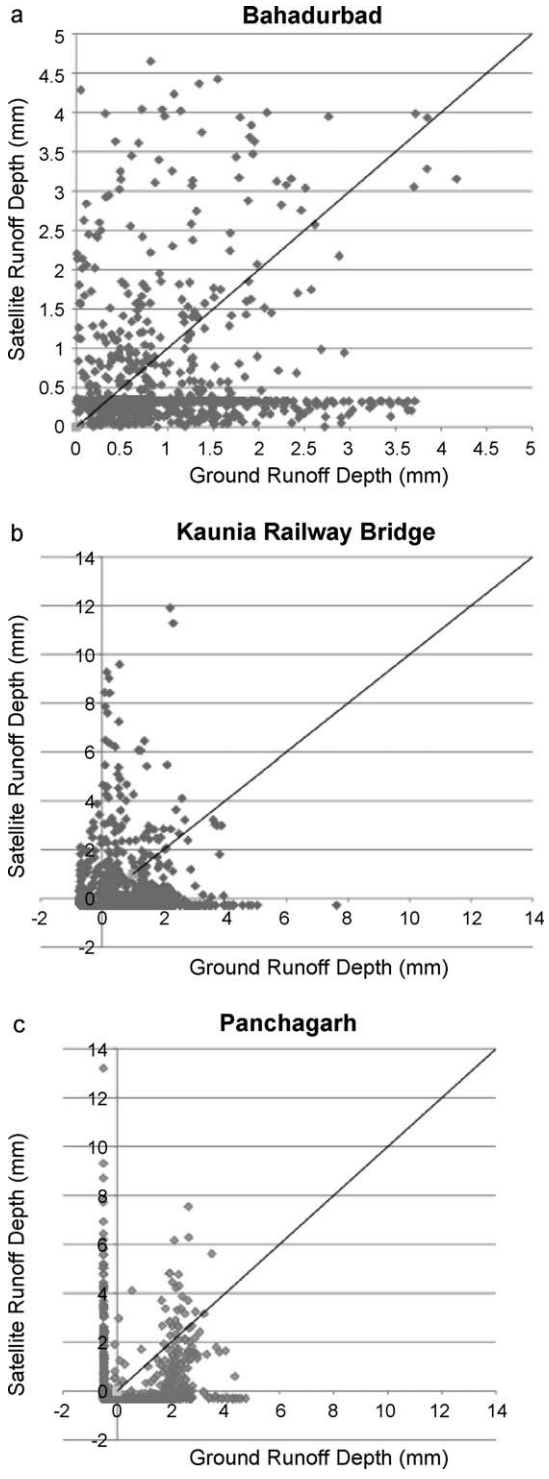

Fig. 14. Scattergrams for the Brahmaputra river basin stations.

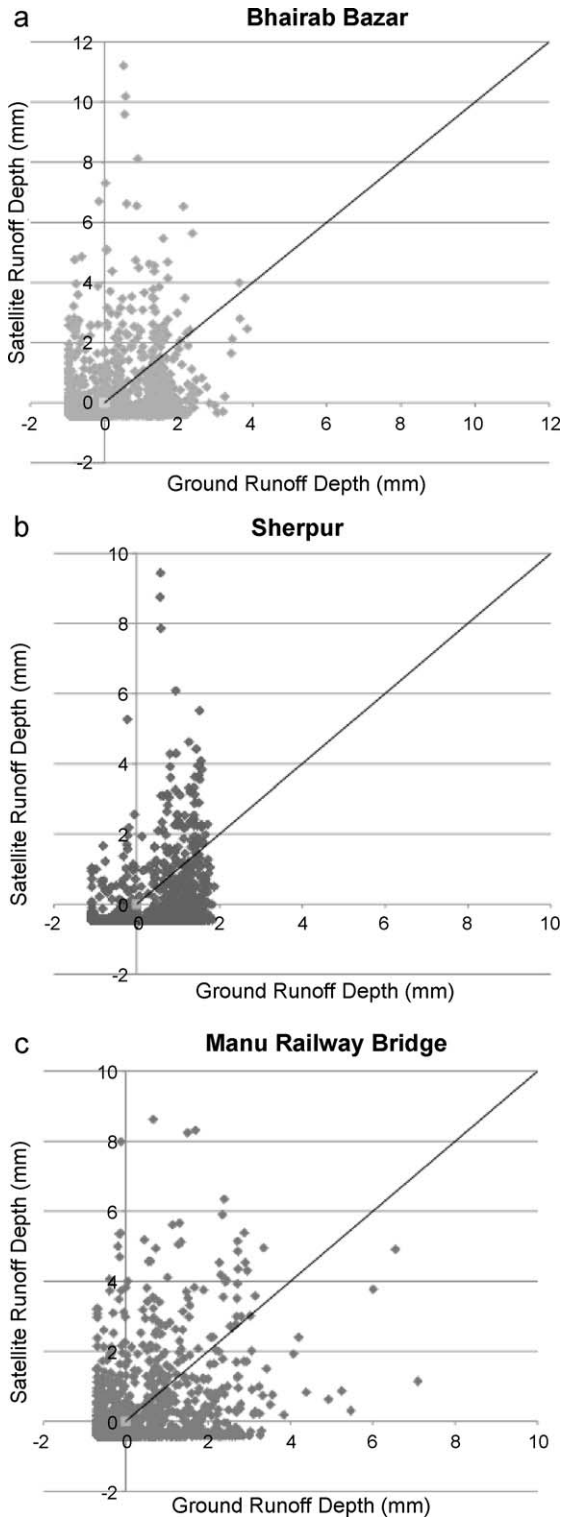

Fig. 15. Scattergrams for the Meghna river basin stations.

When the data was broken into monsoon and non-monsoon seasons, the POD_{rain} increased on average to 0.59 for the monsoon season (Fig. 7), but decreased to 0.51 for the non-monsoon season (Fig. 8). The $POD_{no\ rain}$ decreased on average to 0.63 in the monsoon season and increased to 0.83 in the non-monsoon season. The FAR_{rain} increased on average (0.37) for the monsoon season. This trend appeared to be a commonality with past rainfall validation studies. For example, Su et al. (2008) have shown an increase in false events as the daily precipitation thresholds increased. However, the FAR_{rain} decrease to 0.17 for the non-monsoon season indicated better performance of 3B42V6 during periods of lighter or less frequent rainfall. Habib and Krajewski (2002) reported higher variability in rainfall during periods of heavy rain than of those with light rain. The higher variability of rainfall could contribute to the increased tendency of 3B42V6 to over-detect rainfall during the monsoon season.

Table 4
Unconditional and conditional analysis for TMPA (3B42V6) rainfall data.

	Unconditional			Conditional		
Station	RRMSE	Bias	Correlation	RRMSE	Bias	Correlation
Hardinge Bridge	3.51	0.88	0.27	1.32	0.90	0.17
Gorai Railway Bridge	3.93	0.87	0.19	1.52	0.85	0.05
Bahadurabad	3.55	0.92	0.33	1.60	1.09	0.15
Kaunia Railway Bridge	3.31	0.81	0.39	1.26	0.69	0.32
Panchagarh	2.67	0.58	0.39	1.29	0.56	0.26
Bhairab Bazar	3.32	0.79	0.27	1.42	0.71	0.14
Sherpur	4.35	1.29	0.01	1.66	0.88	0.01
Manu Railway Bridge	2.73	0.93	0.30	1.50	1.00	0.17

The scalar magnitude component of the validation showed that the 3B42V6 underestimated the magnitude of rainfall (Table 4). Overall, the bias showed that the satellite underestimated the ground rainfall data by about 11.6%. Other TRMM-based rainfall validations have in the past shown contrasting results in terms of scalar magnitude of rainfall. For example, Tian et al. (2007) showed that 3B42V6 generally overestimated rainfall for the contiguous United States. Su et al. (2008) reviewed 3B42V6 over the La Plata basin in South America and reported that the agreement between satellite precipitation data and ground data was reduced during high rain rates. Gottschalck et al. (2005) found that TMPA near real-time precipitation estimates overestimated summertime rainfall estimates in the United States. Islam and Uyeda (2000) showed for Bangladesh that, satellite-based products overestimated rainfall during the non-monsoon season, but underestimated rainfall during the monsoon season.

The conditional bias of 3B42V6 was found to be 5.1% lower than the unconditional bias, while the conditional RRMSE (1.45) was lower than the unconditional RRMSE (3.42). These results indicated that the satellite rainfall data had a tendency to sense more accurately the magnitude of rainfall for a "hit" scenario. Results for correlation show that the unconditional correlation (0.27) was higher than the conditional correlation (0.16). These results could be attributed to the large number of non-rainy days in the ground datasets that would increase the unconditional correlation. Though there is a challenge in sensing the magnitude of rainfall, the 3B42V6's ability to sense trends in rainfall, its availability on a near-global scale, and its ready availability makes it a unique data source for global rainfall monitoring.

5.2. Flood potential analysis

The first goal of the flood potential analysis was to determine how well the TMPAV6 estimated trends in and the magnitude of runoff depth on the ground. Overall, the POD_{flood} (0.67) and the $POD_{no\ flood}$ (0.69) were observed to be high, indicating that the system sensed trends in ground runoff depth quite well (Fig. 9). The FAR_{flood} (0.31) was high, appearing to undermine the credibility of flood detection, which could lead to problems with implementing the FDS for disaster management and decision-making among end-users.

For assessing the performance of the FDS in different river basins (Fig. 10), an increased sensitivity in the mountainous Meghna River basin was observed, with a higher POD_{flood} (0.78) and FAR_{flood} (0.40) values than for the Ganges or Brahmaputra Basins (Fig. 10). The

Table 5
Unconditional and conditional analysis for FDS flood potential data.

	Unconditional		Conditional	
Station	Bias	Correlation	Bias	Correlation
Hardinge Bridge	0.12	0.14	0.01	−0.01
Gorai Railway Bridge	−0.56	0.17	0.85	−0.03
Bahadurabad	0.64	0.25	0.93	0.19
Kaunia Railway Bridge	−0.09	0.21	0.42	0.06
Panchagarh	0.27	0.20	0.58	0.29
Bhairab Bazar	0.15	0.24	0.33	0.02
Sherpur	0.43	0.39	0.40	0.14
Manu Railway Bridge	−2.61	0.40	−0.39	0.22

sensitivity could be attributed to the high CN associated with the rocky soil of the mountainous terrain in the NRCS-CN model (Soil Conservation Service, 1986), causing the rainfall to be partitioned more rapidly as runoff. For the regulated Ganges River, the FDS showed the lowest POD_{flood} (0.56), which could be attributed to the runoff generated by rainfall being impounded upstream before being released. The NRCS-CN model has no way of accounting for the impact of hydraulic structures on flow, so its estimates for a regulated river are not as accurate. The FDS performed best for the Brahmaputra River basin with high POD_{flood} (0.75) and $POD_{no\ flood}$ (0.71) and low FAR_{flood} (0.29). This could be attributed to the fact that it is a natural river with no hydraulic structures built along its reach.

Dividing the data into monsoon and non-monsoon season helped determine the effectiveness of the system during periods of high rainfall accumulation. For the monsoon season, the POD_{flood} (0.71) was high indicating that the system picked up on flooding well (Fig. 11). The FAR_{flood} (0.54) was also found to be high, indicating an extreme sensitivity of the system to falsely detect flood during the monsoon season. During the non-monsoon season, the POD_{flood} (0.38) was found to be lower (Fig. 12). The POD_{flood} for Sherpur was zero because five floods occurred and none were detected. The FAR_{flood} of 0.16 was also found lower for the non-monsoon season.

The high FAR rate seen during the monsoon season in the flood potential analysis could be attributed to the higher variability in the rainfall data during that time period. During the monsoon season, high rainfall accumulation creating high flows close to those that trigger the "flood" response in the FDS are more common, thus making it more difficult for the FDS to distinguish between the two. During the non-monsoon season, these flows were lower, and hence, the extreme peaks were more likely to be discriminated well. Our analysis showed that the FDS system could also be well suited for sensing localized flooding to help with disaster management during the non-monsoon season due to the low instances of FAR.

The scalar magnitude component of the flood potential validation showed that the FDS generally underestimated the magnitude of flooding (Table 5). The bias results showed an overall underestimation bias (0.205). The unconditional correlation (0.27) was higher than the conditional correlation (0.12). In general, the performance of the FDS mimicked the trends seen in the assessment of 3B42V6 data against ground data.

The scattergrams showed similar results as all of the river stations show underestimation (Figs. 13–15). Considering the FDS performance by major river basin, the scattergrams showed that the system performs best in the Brahmaputra River basin (Fig. 14) followed by the Meghna River basin (Fig. 15). Both stations in the Ganges River showed underestimation. This could be attributed to the fact that the Brahmaputra and Meghna rivers are more natural streams where the Ganges is regulated.

Although the magnitude of flooding is underestimated using the NRCS-CN runoff depth values, the FDS is effective in sensing the trends in ground runoff depth as shown by the trend analysis for flood potential. As this is the only system of its kind that is available on a near-global scale and in near–near real-time, the flood risk data that is available through the FDS appears quite valuable to countries that do not have the ground infrastructure to monitor flooding. However, improvements to the system are necessary to further enhance the FDS estimation credibility among end-users for disaster management.

To our knowledge, no other validations of the FDS NRCS-CN-based flood potential product exists. It has been suggested that the FDS could perform better using a more complex hydrologic model (Hossain et al., 2007). Li et al. (2008) showed acceptable results using the TMPA-based rainfall products as input for the conceptual, physically-based, distributed Xinanjiang Model for the Nzoia basin in Africa. Su et al. (2008) found results with similar trends to our study using TMPA-based rainfall as an input to the Variable Infiltration Capacity (VIC) model, noting that the TMPA-based simulated flow effectively reads trends in seasonal stream flow variability. The improvement in estimations shown by the more sophisticated models gives hope to the refinement of the FDS if one of these models is implemented into the system in the future.

6. Conclusions

A ground validation of TMPA (3B42V6) rainfall and TRMM-based FDS flood potential data was presented for the flood prone region of Bangladesh that faces transboundary hurdles to ground-based flood forecasting. This validation is important for FDS users and developers to understand the system's performance using the currently implemented hydrologic model and for future improvements through the use of more sophisticated models. Refinement of this system through validation could lead to a more effective and reliable, near real-time flood monitoring system, which could significantly reduce the societal and financial impacts that large-scale flooding has worldwide.

For this study, eight sites were selected within Bangladesh to analyze the performance of the satellite-based 3B42V6 rainfall product for monitoring rainfall and the satellite-based FDS flood potential product for detecting flooding. Overall, the 3B42V6 estimated patterns in rainfall well. Although the FDS was also found effective in detecting patterns in runoff depth, magnitude of the events was generally underestimated. Both 3B42V6 and the FDS showed a higher level of uncertainty during the monsoon season with higher FAR_{flood} values than average. For this reason, FDS users are cautioned to verify FDS estimates with ground observations before implementing flood management practices during this critical monsoon period. The high FAR_{flood} may compromise the credibility of the FDS's flood warnings, so local-scale verification is necessary for end-users to confidently execute steps towards flood disaster management.

Considering the FDS performance in different river basins, the FDS also showed an increased sensitivity to under-predict in the mountainous Meghna River basin because of the high CN associated with the mountainous terrain in the NRCS-CN model. FDS users should therefore consider the topographic and soil features of the basin before implementing flood management practices and verify FDS estimates in mountainous terrain. For the regulated Ganges River, the FDS performed the worst, with the lowest POD_{flood}. This is because the NRCS-CN model has no way of accounting for the impact hydraulic structures on flow, so its estimates for a regulated river are not accurate. The FDS performed best for the Brahmaputra River basin because it is a natural river with no hydraulic structures built along its reach.

Understanding how the FDS performs in Bangladesh can lead to future improvements of the FDS in humid, flood-prone regions in

other parts of the world like Africa, South America, and southeast Asia. New, dynamic, rainfall input from GPM in 2013 and implementation of more sophisticated hydrologic models as described by Li et al. (2008) and Su et al. (2008) are expected to improve the quality of FDS data. Validation work similar to this study will be required to quantify these proposed modifications in the future. In the meantime, an interim goal for a global system should be to work towards the seamless integration of existing Flood Detection Systems such as ITHACA, GFAS, TRMM-FDS and Dartmouth Flood Observatory to provide added value to the users on the ground in flood-prone regions.

Acknowledgments

The ground validation datasets used in this study were available through an agreement between Institute of Water Modeling (Bangladesh) and Tennessee Technological University. This study was supported by the NASA New Investigator Program Award (NNX08AR32G) for author Faisal Hossain.

References

Ahmad, Q.K., Ahmed, A.U., Khan, H.R., Rasheed, K.B.S., 2001. GBM regional water vision: Bangladesh perspectives. In: Ahmad, Q.K., Biswas, A.K., Rangachari, R., Sainju, M.M. (Eds.), Ganges–Brahmaputra–Meghna region: A Framework for Sustainable Development. University Press Limited, Dhaka, pp. 31–78.

Bakker, M.H.N., 2006. Transboundary River Floods: Vulnerability of Continents, International River Basins and Countries. Ph.D. Dissertation. Oregon State University, Corvallis.

Balthrop, C., Hossain, F., 2010. A review of state of the art on treaties in relation to management of transboundary flooding in international river basins and the global precipitation measurement mission. Water Policy, doi:10.2166/wp.2009.117.

Brackenridge, G.R., Nghiem, S.V., Anderson, E., Chien, S., 2010. Space-based measurement of river runoff. EOS 86 (19).

Ebert, E.E., Janowiak, J.E., Kidd, C., 2007. Comparison of near–near real-time precipitation estimates from satellite observations and numerical models. Bulletin of the American Meteorological Society 88, 47–64.

Gottschalck, J., Meng, J., Rodell, M., Houser, P., 2005. Analysis of multiple precipitation products and preliminary assessment of their impact on Global Land Data Assimilation System land surface states. Journal of Hydrometeorology 6, 573–598.

Habib, Emad, Krajewski, W.F., 2002. Uncertainty analysis of the TRMM ground-validation radar-rainfall products: application to the TEFLUN-B field campaign. Journal of Applied Meteorology 41, 558–572.

Hong, Y., Adler, R.F., Hossain, F., Curtis, S., Huffman, G.J., 2007. A first approach to global runoff simulation using satellite rainfall estimation. Water Resour. Res. 43, W08502, doi:10.1029/2006WR005739.

Hong, Y., Adler, R., 2008. Estimation of global SCS curve numbers using satellite remote sensing and geospatial data. International Journal of Remote Sensing 29 (2), 471–477.

Hopson, T.M., Webster, P.J., 2009. A 1–10 day ensemble forecasting scheme for the major river basins of Bangladesh: forecasting severe floods of 2003–2007. Journal of Hydrometeorology, doi:10.1175/2009JHM1006.1.

Hossain, F., Katiyar, N., 2006. Improving Flood Forecasting in International River Basins. EOS (AGU) 87 (5), 49–50.

Hossain, F., Katiyar, N., Hong, Y., Wolf, A., 2007. The emerging role of satellite rainfall data in improving the hydro-political situation of flood monitoring in the under-developed regions of the world. Natural Hazards 43 (2), 199–210, doi:10.1007/s11069-006-9094-x.

Hou, A., Jackson, G.S., Kummerow, C., Shepherd, C.M., 2008. Global precipitation measurement. In: Silas, M. (Ed.), Precipitation: Advances in Measurement, Estimation, and Prediction. Springer Publishers, pp. 1–39.

Huffman, G.J., Adler, R.F., Bolvin, D.T., Gu, G., Nelkin, E.J., Bowman, K.P., Hong, Y., Stocker, E.F., Wolff, D.B., 2007. The TRMM multi-satellite precipitation analysis (TMPA): quasi-global, multi-year, combined-sensor precipitation estimates at fine scales. Journal of Hydrometeorology, doi:10.1007/978-90-481-2915-7_1.

Islam, M.R., Begum, S.F., Yamaguchi, Y., Ogawa, K., 1999. The Ganges and Brahmaputra rivers in Bangladesh: basin denudation and sedimentation. Hydrological Processes 13, 2907–2023.

Islam, M.N., Uyeda, H., 2000. Use of TRMM in determining the climatic characteristics of rainfall over Bangladesh. Remote Sensing of Environment 108 (3), 264–276.

Kera, K., Nagai, M., 2006. Global flood alert system (GFAS) – a new information system utilizing satellite rainfall data to support flood forecasting and warning. In: 4th Annual Mekong Flood Forum, Siem Reap, Cambodia, 18–19 May, p. 2006.

Kummerow, C., Simpson, J., Thiele, O., Barnes, W., Chang, A.T.C., Stocker, E., Adler, R.F., Hou, A., Kakar, R., Wentz, F., Ashcroft, P., Kozu, T., Hong, Y., Okamoto, K., Iguchi, T., Kuroiwa, H., Im, E., Haddad, Z., Huffman, G., Ferrier, B., Olson, W.S., Zipser, E., Smith, E.A., Wilheit, T.T., North, G., Krishnamurti, T., Nakamura, K., 2000. The status of the Tropical Rainfall Measuring Mission (TRMM) after two years in orbit. Journal of Applied Meteorology 39, 1965–1982.

Li, L., Hong, Y., Wang, J., Adler, R.F., Policelli, R.S., Habib, S., Irwn, D., Korme, T., Okello, L., 2008. Evaluation of the near real-time TRMM-based multi-satellite precipitation analysis for an operational flood prediction system in Nzoia Basin, Lake Victoria, Africa. Natural Hazards, doi:10.1007/s11069-008-9324-5.

Paudyal, G.N., 2002. Forecasting and warning of water-related disaster in a complex hydraulic setting: the case of Bangladesh. Hydrological Sciences Journal 47, S5–S18 (S).

Rahaman, M.M., 2005. Bangladesh – from a country of flood to a country of water scarcity – sustainable perspectives for solution. In: Seminar on Environment and Development. Entwicklungsforum, Hamburg, Germany.

Simpson, J., Adler, R.F., North, G.R., 1988. A proposed Tropical Rainfall Measuring Mission (TRMM) satellite. Bulletin of the American Meteorological Society 69, 278–295.

Soil Conservation Service, 1986. Urban Hydrology for Small Watersheds. Technical Release 55. U.S. Department of Agriculture, Washington, DC.

Stokstad, E., 1999. Scarcity of rain, stream gages threatens forecasts. Science 285, 1199.

Su, F., Hong, Y., Lettenmaier, D.P., 2008. Evaluation of TRMM Multisatellite Precipitation Analysis (TMPA) and its utility in hydrologic prediction in the La Plata Basin. Journal of Hydrometeorology 9, 622–640.

Tian, Y., Peters-Lidard, C., Choudhury, B., Garcia, M., 2007. Multitemporal analysis of TRMM-based satellite precipitation products for land data assimilation applications. Journal of Hydrometeorology 8, 1165–1183.

Wahl, K.L., Thomas Jr., W.O., Hirsch, R.M., 1995. Stream-Gauging Program of the U.S. Geological Survey. U.S. Geological Survey Circular 1123, Reston, VA.

World Water Assessment Programme, 2009. The United Nations World Water Development Report 3: Water in a Changing World. UNESCO, Earthscan, Paris, London.